JOURNAL OF AGRICULTURAL AND FOOD CHEMISTRY

REVIEWS

Glass Transition and Enthalpy Relaxation of Amorphous Food Saccharides: A Review

YETING LIU,† BHESH BHANDARI,§ AND WEIBIAO ZHOU*,†

Food Science and Technology Programme, c/o Department of Chemistry, National University of Singapore, Science Drive 4, Singapore 117543, and School of Land and Food Sciences, The University of Queensland, Brisbane, QLD 4072, Australia

Many food materials exist in a disordered amorphous solid state due to processing. Therefore, understanding the concept of amorphous state, its important phase transition (i.e., glass transition), and the related phenomena (e.g., enthalpy relaxation) is important to food scientists. Food saccharides, including mono-, di-, oligo-, and polysaccharides, are among the most important major components in food. Focusing on the food saccharides, this review covers important topics related to amorphous solids, including the concept and molecular arrangement of amorphous solid, the formation of amorphous food saccharides, the concept of glass transition and enthalpy relaxation, physical property changes and molecular mobility around the glass transition, measurement of the glass transition and enthalpy relaxation, their mathematical descriptions and models, and influences on food stability.

Keywords: Amorphous solid; glass transition; enthalpy relaxation; food saccharides; DSC

1. INTRODUCTION

Unlike crystalline structure, the amorphous or glassy state has a kinetically nonequilibrium structure. Many food materials exist in a completely or partially amorphous state due to food processing (*1*−*5*). An amorphous solid has a liquid-like structure with a viscosity $>10^{12}$ Pa•s (*1*). Glass transition refers to the phase transition when a glass is changed into a supercooled melt or the reverse (*5*). Rapid changes in the physical, mechanical, electrical, thermal, and other properties of a material can be observed through the glass transition (*6*); these changes are described by mathematical expressions such as Vogel−Tamman−Fulcher (VTF) and Williams−Landel−Ferry (WLF) equations. Through the measurement of those rapidly changed properties, the glass transition temperature can be determined. Mathematical models, described by the Gordon−Taylor and Couchman−Karasz equations, are able to predict the glass transition temperature of multicomponent mixtures. Although the glass transition temperature has been proven to be an effective indicator for food quality changes during storage (*5*−*7*), there is evidence that physicochemical changes also take place below the glass transition temperature (*8*).

When a glassy material is stored below its glass transition temperature, it spontaneously approaches a more stable state (*9*). This phenomenon is called enthalpy relaxation, which is due to the local molecular motion of certain molecules or certain parts of some polymer molecules (*10*). The enthalpy relaxation is both nonexponential and nonlinear (*5*). Such characteristics are described by Kohlrausch−Williams−Watts (KWW) and Tool−Narayanaswamy−Moynihan (TNM) expressions. Although the enthalpy relaxation is of molecular origin, it is accompanied by changes in macroscopic properties (*8*), such as density, mechanical properties, and transport properties. Enthalpy relaxation is important for food materials stored below the glass transition temperature, in consideration of the stability of the physicochemical properties of the materials.

In this review, all of the above topics are discussed with emphasis on food saccharides, one of the most important major components of processed foods. The next section covers the concept of amorphous solids, their molecular arrangement, and amorphous food solids. Glass transition and its related topics, including molecular mobility, physical property change, measurement, prediction model, and its influence on food stability will be discussed in section 3. Enthalpy relaxation and its related topics, such as its characteristics, measurement, and its influence on food stability, will be presented in section 4.

2. AMORPHOUS SOLIDS

2.1. Concept of Amorphous State. Gas, liquid, and solid are the three commonly known states in nature. They differ mainly in molecular mobility. Among them, the solid state has the lowest molecular mobility because its molecules are fixed at their own positions. The crystalline state is a well-known solid state having molecules well arranged in a regular lattice.

* Corresponding author [telephone (65) 6516-3501; fax (65) 6775-7895; e-mail chmzwb@nus.edu.sg].
† Food Science & Technology Programme, c/o Department of Chemistry, National University of Singapore, Science Drive 4, Singapore 117543
§ School of Land and Food Sciences, The University of Queensland, Brisbane QLD 4072, Australia

10.1021/jf060188r CCC: $33.50
Published on Web 07/13/2006

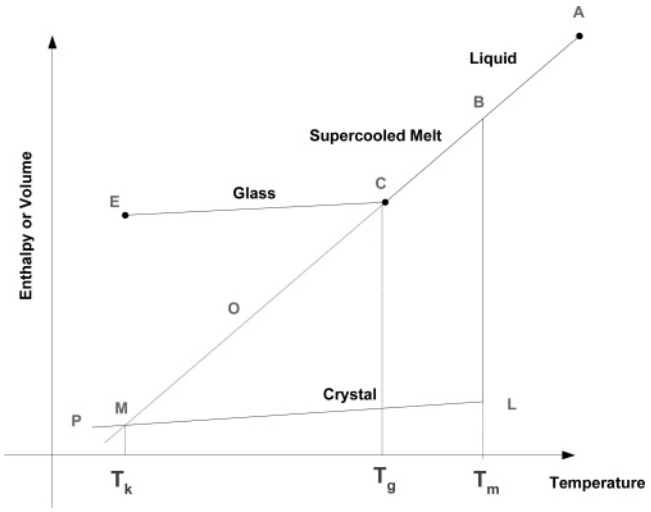

Figure 1. Illustration of formation of amorphous solids by rapid cooling.

Besides the crystalline state, solids could exist in another state called the amorphous or glassy state, the molecular arrangement of which is disordered with reference to the crystalline state.

Amorphous solids are commonly formed through rapid cooling of a liquid melt to a certain temperature so that the molecules in the melt do not have enough time to rearrange and are frozen in their original position. The formed amorphous solid has a liquid-like structure but in the solid phase. An amorphous solid is also called a glass, and it is characterized by its liquid-like structure with an extremely high viscosity.

When a liquid is slowly cooled below its melting point, crystals will usually form and the liquid solidifies, indicated by line ABLM in **Figure 1**. Sometimes it can remain as a liquid below its melting point if there is no nucleation site to initiate the crystallization process (line BC in **Figure 1**). If, during cooling, the viscosity (resistance to flow) of the supercooled liquid increases rapidly and continuously, then the liquid will never crystallize and it forms an amorphous solid (line CE in **Figure 1**), having molecules that are disordered and cohesive enough to maintain rigidity. If the supercooled melt is allowed to remain as a liquid as the temperature decreases (line CO), the extrapolation of the liquid line (line ACO) will cross with the crystalline line (line LP) at point M, the corresponding temperature of which is T_k, the Kauzmann temperature. Below T_k, the enthalpy of the supercooled liquid is lower than that of its crystalline solid, and the liquid is more ordered than the solid. This is not possible as the order of liquid cannot be higher than that of crystalline solid and, thus, is called Kauzmann's paradox (*11*). This paradox is avoided in practice because, prior to T_k, the supercooled liquid has changed into an amorphous solid.

2.2. Molecular Arrangement of Amorphous Solids. A liquid to crystal transition is a thermodynamic process, as the crystal state is energetically more favorable than the liquid below the melting point. Glass formation is purely kinetic, where the disordered glassy state does not have enough kinetic energy to overcome the potential energy barriers required for the movement of its molecules to pass one another. The molecules of the glass take on a fixed but disordered arrangement.

The molecular arrangement of an amorphous solid (**Figure 2**) can be described with reference to a crystalline solid, which has a molecular arrangement that is a regular lattice. Although the arrangement in the amorphous solid is disordered, it can have short-range molecular order (*9*) similar to that in a crystalline solid. For example, a single molecule in the amorphous solid, compared to that in the crystalline solid, has

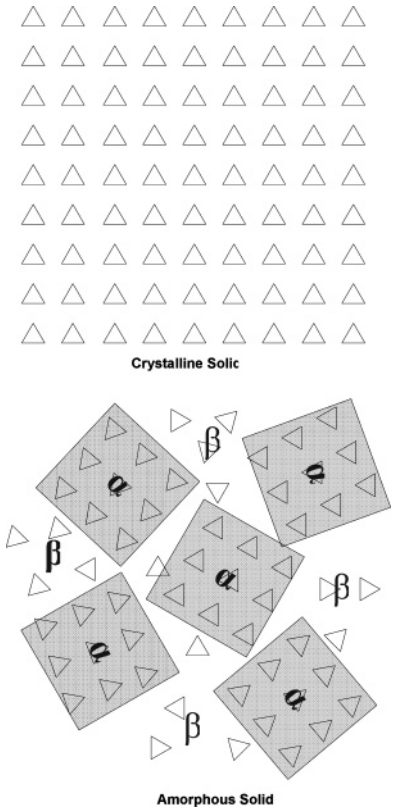

Figure 2. Structure of an amorphous solid. In the amorphous solid, the microheterogeneity is presented as the shaded high-density α regions and the nonshaded low-density β regions.

a similar number of neighbor molecules and a similar distance to the nearest neighbor molecule. However, this similar short-range molecular order is only over a few molecular dimensions (*1*) and quantified as a few angstroms (*12*). However, the surrounding environment of a molecule in the glass may not be significantly different from that in the crystal. Unlike the crystalline solid, the amorphous solid lacks the long-range order of molecular packing (*9*). In other words, the amorphous solid does not have long-range translational orientational symmetry that characterizes a crystal. An amorphous solid may have distinct regions and, therefore, microheterogeneity (*13*, *14*), such as high-density α regions and low-density β regions, which are between high-density α regions (**Figure 2**).

As an example, the heterogeneity of the amorphous state could be found in native starch, which occurs in the form of discrete granular particles. Starch granules are composed essentially of amylose and amylopectin. They are heterogeneous, exhibiting a wide distribution of molecular structures and sizes. For granular starch, its growth rings consist of alternating crystalline (double-stranded helices of short chains of amylopectin) and amorphous lamellae, according to Biliaderis (*15*). The crystalline and amorphous lamellae of amylopectin are organized into larger and more or less spherical "blocklets". These blocklets contain short chains of amylopectin clusters. As suggested by Biliaderis (*15*), with this type of granular organization, amorphous material may exist in different regions: (1) in each lamella (branching zones of the amylopectin); (2) between clusters of side chains within each lamella; (3) around each blocklet of side-chain clusters; (4) in radially arranged channels in granules through which amylose can exit (leach out) during gelatinization. Amorphous material is a major portion of granular starch. Amylose molecules do not exist in the form of bundles in amorphous regions, but rather are

interspersed among the amylopectin molecules. In the study by Chung and Lim (*16*), dual glass transitions were observed in normal rice starch, which indicated that the amorphous regions in the normal rice starch were heterogeneous. As suggested by the authors, the heterogeneity in the normal rice starch might result from the interaction between crystalline and amorphous regions, which induced different amorphous regions including less restricted and more restricted, and these different amorphous regions behaved differently and resulted in dual glass transitions.

In general, an amorphous solid has a kinetically frozen liquid-like structure, formed by rapid cooling of a melt below its melting temperature. In a glass, the translational motion and rotational motion of the molecules are reduced to a point of practical insignificance (*17*). For example, the long-range thermal motion of individual molecules of small molecular weight materials is frozen out, and the wriggling motion of long chains of polymers is also frozen out, leaving the chains locked into an entangled mass (*12*). Therefore, the Stokes viscosity (local viscosity, not the bulk viscosity) is appropriate for characterizing glasses (*17*). Of course, the vibrational mobility does not cease until absolute zero temperature is achieved.

2.3. Amorphous Food Solid Materials. Amorphous solids exist in many individually important products, such as polymers, ceramics, metals, optical materials (glasses and fibers), foods, and pharmaceuticals (*9*). Many food-processing techniques involve phase changes. The phase changes of food components may cause the partial or complete destruction of an organized molecular structure to a disorganized structure, which forms an amorphous structure. The development of an amorphous food structure could result from melting, denaturation, glass transition, gelatinization, mechanical shear, rapid removal of dispersing solvent, and depolymerization of large structure. Familiar routes to an amorphous state include drying, such as spray-drying (*18*) and hot air-drying (*2*); freezing, such as rapid cooling (*1*) and freeze-drying (*3*); grinding, such as ball-milling (*4*); extrusion (*5*), etc. In a word, many processed food materials exist in an amorphous state, such as hard candy and many food powders: dairy, instant coffee and tea, protein, cheese, spice, cocoa, etc.

The amorphous state is not a thermodynamic equilibrium state (*17*), as the crystalline state is the favorable low-energy state for a material below its melting point. There are two major transitions in amorphous solids, glass transition and enthalpy relaxation. They both relate to the changes in quality and physical properties of amorphous food products during storage (*19*).

3. GLASS TRANSITION

3.1. Concept of Glass Transition. There are two groups of phase transitions in foods: first-order phase transition and second-order phase transition. They are differentiated by the latent heat, which is the heat flowing to or from a material without change of its temperature. The commonly known phase transitions, such as crystallization, melting, condensation, and evaporation, are all first-order phase transitions, which are characterized by the release or absorption of latent heat during the physical state change isothermally from one state to another, such as liquid to solid, solid to liquid, and gas to liquid. In terms of latent heat, glass transition is often referred as a second-order phase transition that occurs without the release or absorption of latent heat. However, due to the nonequilibrium nature of the glass, glass transition is preferably called a state transition, rather than a phase transition (*20*). Due to the other features of the glass transition, such as its occurrence over a temperature range and the dependence of its determination on experimental conditions, it is also preferably called a kinetic and relaxation transition, rather than a second-order transition (*20*). The characteristics of glass and glass transition, such as those just mentioned, will be discussed more in the later sections. The various physical states of materials are illustrated in **Figure 3**.

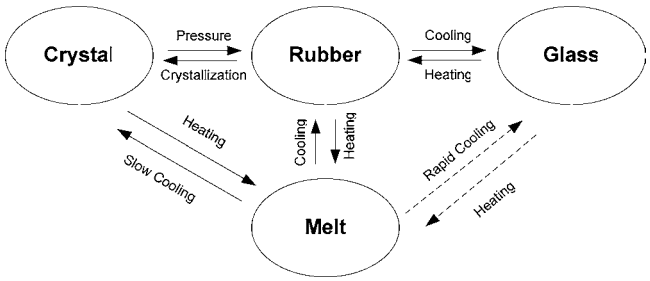

Figure 3. Physical states of materials (modified from ref *6*).

Glass transition, or glass−liquid transition (GLT), is a name given to the phenomenon observed when a glass is changed into a supercooled liquid, or to the reverse transformation (*5*). These reversible transformations between supercooled liquid and glass are usually brought about by heating and cooling (*3*, *5*, *6*). The glass and supercooled liquid differ in their molecular mobilities, that is, short-range vibration and rotation in glass, and long-range translation and rotation in supercooled liquid (*20*). Besides heating and cooling, the transformation between supercooled liquid and glass can also be achieved by increasing the material's water content to convert glass to supercooled liquid (such as water absorption) and by decreasing the water content to convert supercooled liquid to glass (such as rapid evaporation), due to the significant plasticizing effect of water (plasticizing effect will be discussed later in section 3.5). Schmidt (*20*) suggested such transformations between glass and supercooled liquid be called glass transition as well. However, during those transformations, the chemical composition or nature of the material/glass has been changed due to the addition or removal of water. Therefore, rigorously speaking, the sample under test is no longer the same material. In this paper, we focus on the physical transitions of materials for which the compositions do not change during the transition, and the glass transition caused by changing water content is excluded.

The glass transition temperature (T_g) is defined as the temperature range corresponding to the glass−liquid transition. Both the glass and the supercooled melt are in the noncrystalline state. In contrast to the glass that is a rigid solid, the supercooled melt, between T_g and T_m (melting temperature), can be a viscoelastic "rubber" in the case of polymer materials, or a mainly viscous liquid for low molecular weight materials. Unlike T_m, T_g is a kinetic parameter, depending on the temperature scanning rate and the sample's thermal history. Nonetheless, T_g is a useful material descriptor owing to its good correlation with the structural and thermodynamic properties of the material. The glass transition temperatures of some common food saccharides are shown in **Table 1**. The experimental consideration for T_g determination will be addressed in section 3.4.

Currently, knowledge about the glass transition in foods is mainly phenomenological; very little is known about its theoretical aspects (*7*). Compared to amorphous nonfood materials including mineral glasses, natural and synthetic polymers, amorphous food products and ingredients appear to have similar essential features. However food materials are also very different from those for two reasons: (1) the frequent heterogeneity in chemical composition and (2) the predominant role of water as a plasticizer (*7*).

Table 1. Glass Transition Temperature (Midpoint) of Common Anhydrous Food Saccharides[a]

food saccharide	T_g[b] (°C)	thermal history (processed in DSC unless specified otherwise)	ref
fructose	7.47 ± 0.59	anhydrous crystals were heated to 160 °C at 20 °C/min for complete melting and then cooled to 60 °C below their T_g at –20 °C/min	our laboratory
	7[c]	sample was heated to 167 °C at 50 °C/min and then cooled to –33 °C at –50 °C/min	*22*
	6.79 ± 1.07	anhydrous crystals were heated to 168 °C at 10 °C/min and held for 0.3 min; sample was then cooled to below its T_g for physical aging; after aging, sample was heated to 120 °C and held for 10 min; sample was then cooled to 55 °C below its T_g	*23*
	5.30 ± 0.25	anhydrous crystals were heated to 168.2 °C at 10 °C/min and held for 0.3 min; after that, sample was cooled to 55 °C below its T_g	*24*
xylose	13[c]	same as that for fructose in ref *22*, as described above	*22*
glucose	38[c]	same as that for fructose in ref *22*, as described above	*22*
	35.42 ± 0.30	anhydrous crystals were heated to 180 °C at 20 °C/min for complete melting and then cooled to 60 °C below their T_g at –20 °C/min	our laboratory
	37.94 ± 0.73	same as that for fructose in ref *23*, as described above	*23*
	37.07 ± 1.19	same as that for fructose in ref *24*, as described above	*24*
maltose	41.2 ± 0.10	crystals (≈5% w/w moisture) were heated to 140 °C and held for 4 min for melting and then quench-cooled (≈ –100 °C/min) to –20 °C	*25*
sucrose	74[c]	10% w/v aqueous solution was held in a freeze-dryer at –45 °C for 72 h; then the dryer was evacuated to a pressure of ≤50 mTorr; after that, the shelf temperature was raised successively to –35 °C for 24 h, –30 °C for 24 h, –20 °C for 24 h, –10 °C for 12 h, 0 °C for 12 h, 25 °C for 24 h, and 60 °C for 48 h	*26*
	70[c]	same as that for fructose in ref *22*, as described above	*22*
	69.70 ± 0.34	anhydrous crystals were heated to 200 °C at 20 °C/min for complete melting and then cooled to 60 °C below its T_g at –20 °C/min	our laboratory
glucose syrup solid (DE = 42)	81.28 ± 2.16	same as that for sucrose from our laboratory, as described above	our laboratory
raffinose	102[c]	10% w/v aqueous solution was held in a freeze-dryer at –45 °C for 2 h; then the dryer was evacuated to a pressure of ≤50 mTorr; the solution was held at –45 °C for another 8 h; after that, the shelf temperature was raised successively to –30 °C for 24 h, –20 °C for 6 h, 0 °C for 24 h, 25 °C for 24 h, and 60 °C for 48 h	*26*
lactose	108[c]	same as that for sucrose in ref *26*, as described above	*26*
trehalose	115[c]	10% w/v aqueous solution was held in a freeze-dryer at –45 °C for 2 h; then the dryer was evacuated to a pressure of ≤50 mTorr; the solution was held at –45 °C for another 8 h; after that, the shelf temperature was raised successively to –32 °C for 24 h, –20 °C for 8 h, –10 °C for 2 h, –5 °C for 4 h, 25 °C for 24 h, and 60 °C for 48 h	*26*
dextran	229[c]	same as that for sucrose in ref *26*, as described above	*28*
starch	243[c]	not applicable; T_g was obtained from theoretical calculation based on experimental data and the Fox and Flory equation	*29*

[a] The scanning rate for determining the glass transition temperature was 10 °C/min for all data. [b] T_g values are listed as mean ± standard deviation of T_g midpoint only. [c] Standard deviation was not available in the original reference.

3.2. Molecular Mobility at Glass Transition Temperature. In the context of food stability, as vibrational mobility is not of concern, molecular mobility (Mm) generally refers to either translational motion or rotational motion of the molecules (*17*). Below the glass transition temperature of a material, generally, the molecules lose their translational mobility and retain only limited rotational and vibrational mobility. However, in some glassy materials formed by big molecules, such as starch or protein, there may be some small molecules, such as water, that retain certain translational mobility.

The only stable thermodynamic equilibrium state or the true equilibrium state below melting temperature is the crystalline state. A supercooled melt below the melting temperature is only in a metastable state, which is apparent equilibrium or pseudo-equilibrium over the practical time unless sufficient activation energy is provided to overcome the energy barrier and bring it to a new equilibrium state with lower free energy. The enthalpy of a supercooled melt varies as temperature decreases, due to the fact that over the life of measurement, the sample can explore all possible configurations (ergodicity) (*12*). The glass state is an out-of-equilibrium state as well. It has a liquid-like structure similar to that of a supercooled melt, but this liquid-like structure is frozen as a result of a too long relaxation time (nonergodicity), but when the material is stored at a temperature below but close to T_g, a slow evolution of the microstructure can be observed (*12*).

The characteristic time of mobility, τ_{mol}, also called relaxation time, is the time that is necessary for the recovery of equilibrium conditions after perturbation of one property of the materials (*7*). The relaxation time can be calculated from the phenomenological equation describing the rheological properties of highly viscous liquids developed by Maxwell−Kelvin−Voigt (*7*) where η is viscosity. G^*_∞ is the factor of proportionality; it

$$\tau_{mol} = \frac{\eta}{G^*_\infty}$$

has the same dimension as the modulus of elasticity and corresponds to the value of the modulus at infinite frequency. On the basis of the concept of relaxation, the glass−liquid transition region is the temperature range at which this relaxation time of the material is similar to that at the experimental scale (*7*). The glass transition is a kinetic and relaxation process associated with the primary relaxation of material (α relaxation) that corresponds to highly cooperative global motion (translational) of the matrix molecules. This kinetic relaxation is

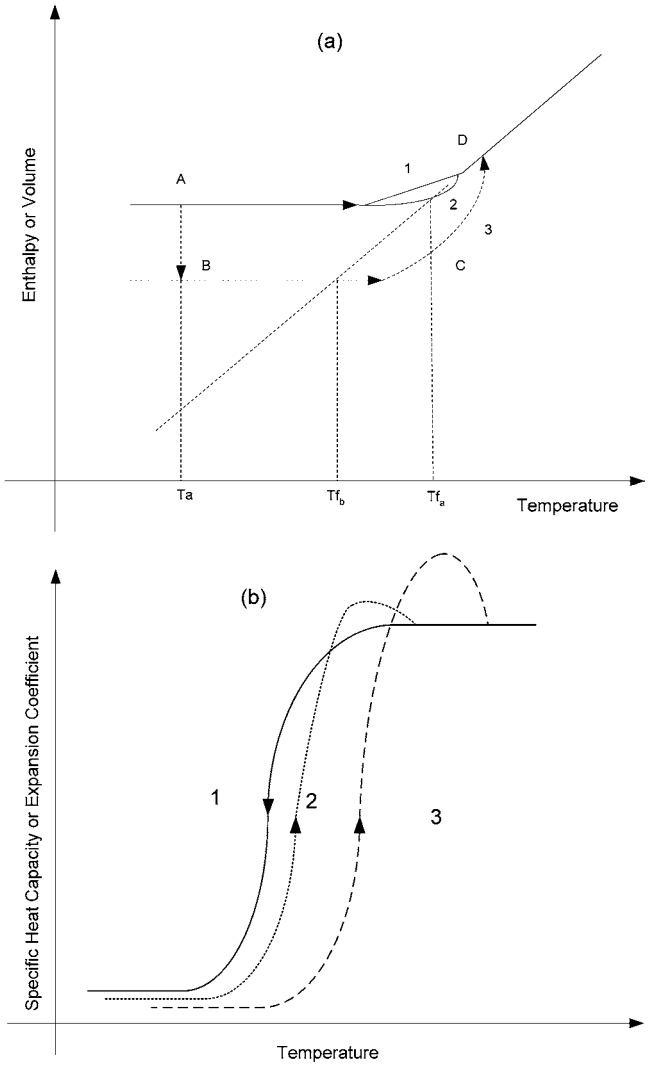

Figure 4. Changes of thermodynamic properties at glass transition temperature. Line 1 refers to the glass transition region when cooling from supercooled melt to glass. Line 2 refers to the glass transition region when reheating from glass to supercooled melt without physical aging. Line 3 refers to reheating from glass to supercooled melt after physical aging. In part **a**, the enthalpy or volume increases or decreases suddenly when the glass is heated or cooled through the glass transition range. In part **b**, there is a step change in the heat capacity or expansion coefficient over the glass transition.

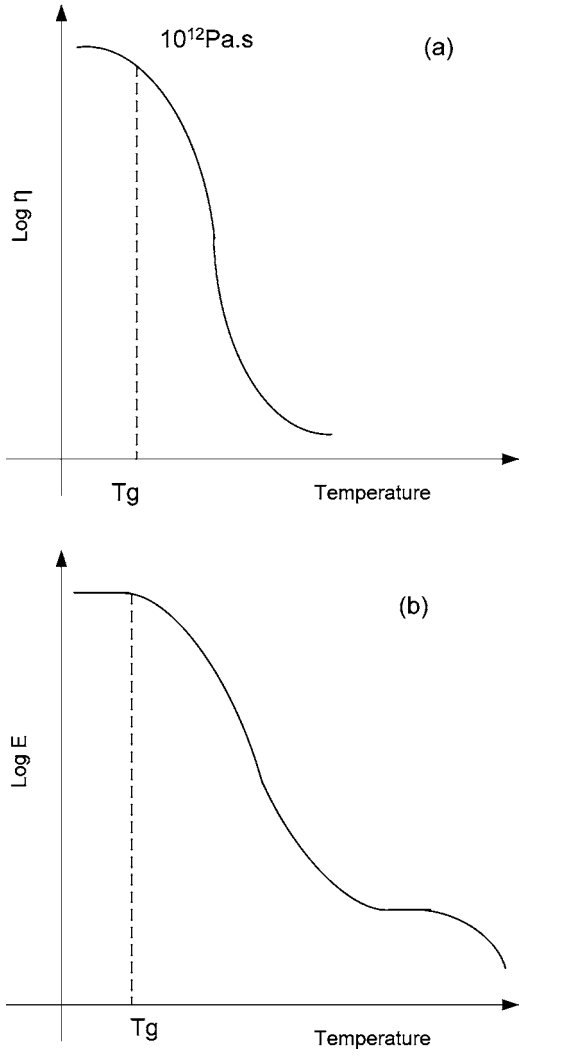

Figure 5. Changes of rheological properties at glass transition temperature.

demonstrated by the fact that T_g is raised when the cooling rate is increased during the creation of a glass through fast cooling of a supercooled melt.

The sensitivity of the relaxation process to temperature depends on the type of molecular motions concerned. This dependence can be characterized with apparent activation energy (E_a), which corresponds to the minimum interaction energy between the molecules. In a supercooled melt, besides the temperature effect on the change of free volume between the molecules, there is also an increase in the interaction energy, including co-operative motions of the molecules. The apparent activation energy is therefore under the influence of both change with temperature of the intermolecular interactions and variation of the free volume (*7*). In a supercooled melt, the apparent activation energy increases as the temperature decreases, reaching high value when it is close to T_g. It commonly attains 200−400 kJ/mol (*5*).

3.3. Physical Property Changes at the Glass Transition Temperature. The glass transition phenomenon is generally characterized by a rapid change in the physical, mechanical, electrical, thermal, and other properties of a material (*6*). When the temperature increases from below to above the glass transition temperature, many of the physical properties of the material suddenly change, including increases in the free volume, heat capacity, thermal expansion coefficient, and dielectric coefficient and changes in the viscoelastic properties (*30*). Free volume is the space not occupied by molecules, which can be thought as the "elbow room" that molecules require to undergo vibrational, rotational, and translational motion (*17*).

Generally, at the glass transition temperature, there are changes in two groups of physical properties: rheological properties (viscosity and modulus) and thermodynamic properties (enthalpy, volume, heat capacity, and expansion coefficient). Therefore, measurement techniques of the glass transition temperature based on those properties' changes generally fall into two groups, and they induce different practical glass transition temperatures. Some of those changes are shown in **Figures 4** and **5**.

Figure 4 illustrates the thermodynamic property changes of a glass formed by rapid cooling of a melt. Line 1 refers to the glass transition region when cooling from supercooled melt to glass. Line 2 refers to the glass transition region when reheating from glass to supercooled melt without physical aging (physical

aging will be discussed in section 4). Line 3 refers to reheating from glass to supercooled melt after physical aging. As shown in **Figure 4a**, the enthalpy or volume increases or decreases suddenly when the glass is heated or cooled through the glass transition range, and there is a step change in the heat capacity or expansion coefficient over the glass transition.

Figure 5b indicates changes in the Young's modulus (E) through the glass transition range. Changes in viscosity during the glass transition are shown in **Figure 5a**. The temperature dependence of viscosity below the glass transition temperature T_g can be described by Arrhenius law:

$$\eta = \eta_0 \exp\left(\frac{E_a}{RT}\right) \quad (1)$$

For a supercooled melt, the flow behavior is no longer Arrhenius-like, and its mechanical properties are strongly dependent on temperature where the temperature coefficient increases as temperature decreases. The most popular expressions are Vogel−Tamman−Fulcher (VTF) (eq 2) and Williams−Landel−Ferry (WLF) (eq 3) equations

$$\eta = \eta_0 \exp\left(\frac{B}{T - T_0}\right) \quad (2)$$

$$\log\left(\frac{\eta}{\eta_{Tg}}\right) = -\frac{C_1(T - T_g)}{C_2 + (T - T_g)} \quad (3)$$

where η and η_{Tg} are viscosities at T and T_g, respectively; η_0, B, T_0, C_1, and C_2 are phenomenological coefficients. Both expressions can be interconverted according to the following relationships between the coefficients ($B' = B/\ln 10$):

$$C_1 = \frac{B'}{T_g - T_0} = \frac{B}{(T_g - T_0)\ln 10}$$

$$C_2 = T_g - T_0$$

In addition, the VTF and WLF expressions can also be applicable to τ_{mol} obtained with, for example, mechanical spectroscopy. When the temperature dependence of molecular motion is described by the VTF equation, the molecular relaxation time τ is involved

$$\tau = \tau_0 \exp\left(\frac{D}{T - T_0}\right) \quad (4)$$

where D, T_0, and τ_0 are constants. The value of T_0 in the VTF equation is believed to correspond to the theoretical Kauzmann temperature (T_k), and τ_0 can be related to the relaxation time constant. The Kauzmann temperature T_k is the critical temperature marking the lower limit of the experimental glass transition temperature, and at T_k the configurational entropy of the system reaches 0 (*1*). When T_0 is 0, the familiar Arrhenius equation is obtained, and D is directly proportional to the activation energy for molecular motion. When $T_0 > 0$, there is a temperature-dependent apparent activation energy (*1*).

C_1 and C_2 in the WLF equation can fluctuate slightly around the "universal" values given by Williams et al. (*31*) ($C_1 = 17.4$ and $C_2 = 51.6$) as a function of the considered material. According to Angell et al. (*32*), this is probably true for C_1 ($C_1 \approx 17$ if the expression is used for the variation of viscosity or 16 if it is applied to the relaxation time), but not for C_2. The variation of C_2 corresponds to the classification proposed by Angell (*33*) to strong/fragile materials according to the variation of their dynamic properties through the glass transition.

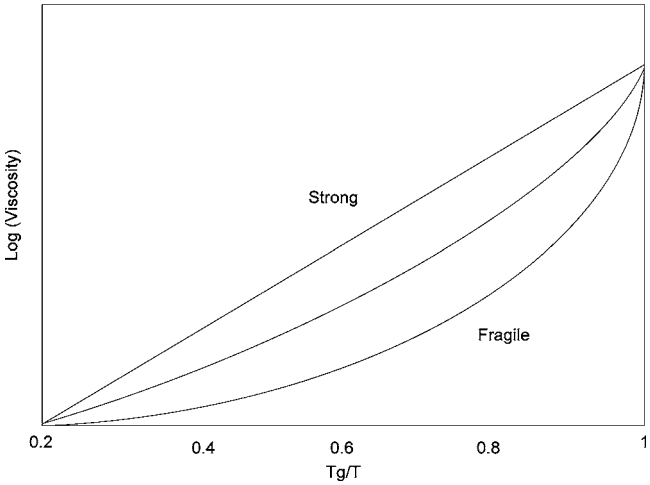

Figure 6. "Angell plot" illustrating the strong (Arrhenius type) and fragile (non-Arrhenius type) liquid behavior.

The fragility parameter m was introduced to differentiate fragile systems from strong ones. By definition, m is the slope of the scaled Arrhenius plot of viscosity when the temperature approaches T_g from above. This parameter m can be calculated from the VTF and WLF coefficients (*5*):

$$m = C_1 + \frac{C_1^2 T_0 \ln 10}{B} \quad \text{or} \quad m = \frac{C_1}{C_2} T_g$$

As mentioned above, C_1 approximates to 17 if the expression is used for the variation of viscosity or 16 if it is applied to the relaxation time. Therefore, the calculation is simplified to

$$m = 16 + \frac{590 T_0}{B} \text{ (for a relaxation time study)}$$

or

$$m = 17 + \frac{666 T_0}{B} \text{ (for a viscosity study)}$$

According to its definition, m can also be expressed as

$$m = \frac{E_a}{RT_g \ln 10}$$

where E_a is the apparent activation energy (kJ/mol). Alternatively, m can be calculated through the DSC measurement of T_g (*34*).

According to Hancock and Zografi (*1*), a strong liquid ($16 < m < 100$) typically exhibits Arrhenius-like behavior or weak temperature dependence of the molecular mobility, but a fragile liquid ($100 < m < 200$) has a much stronger temperature dependence of the molecular mobility near T_g. Meanwhile, a strong liquid has a relatively small change in the heat capacity at T_g, whereas a weak liquid has a relatively large change. In other words, compared to strong liquids, the molecular mobility in fragile liquids changes more rapidly with temperature near T_g; therefore, its molecular arrangement or its configuration structure is broken down more rapidly as well. An "Angell plot" is used to illustrate the difference between two liquids (**Figure 6**). In general, compared to high molecular weight materials, lower molecular weight materials form a more fragile glass.

Table 2. Melting Peak Temperature and the Corresponding Thermal Degradation Temperature at Different Heating Rates for Sucrose, Glucose, and Fructose (Data Adapted from Reference *36*)

sugar	rate of heating (°C/min)	melting temperature (°C)	thermal degradation temperature (°C)
sucrose	0.5	182.7	167.0
	1	186.6	171.3
	2	189.3	178.8
	10	191.5	189.2
	20	192.9	200.7
	50	196.1	214.9
	100	196.5	228.4
glucose	0.5	147.5	147.0
	1	149.3	152.0
	2	151.9	159.0
	10	159.4	170.3
	20	163.8	183.5
	50	168.9	201.1
	100	173.8	204.3
fructose	0.5	113.0	110.4
	1	116.7	113.9
	2	121.0	119.0
	10	131.7	136.8
	20	136.0	147.1
	50	139.8	157.0
	100	142.0	165.4

Table 3. Glass Transition Temperature of Amorphous Sucrose with Various Moisture Contents

moisture content (%)	sucrose T_g (°C)	
	measured[a]	predicted[b]
0	74	74
0.99	60	68
1.47	58	65
1.98	50	62
3.13	32	55

[a] Data from ref *26*. [b] The predicted values were calculated on the basis of the Couchman–Karasz equation using T_g and ΔC_p values of amorphous sucrose and amorphous water. Amorphous sucrose: $T_g = 74$ °C, $\Delta C_p = 0.64$ J/(g·°C). Amorphous water: $T_g = -139$ °C, $\Delta C_p = 1.94$ J/(g·°C).

3.4. Measurement of the Glass Transition Temperature of Food Saccharides. As mentioned in the previous section, there is an abrupt change in several properties of the material in the glass transition range. All of them could be used for the determination of T_g. Generally, T_g is determined by differential scanning calorimetry (DSC) measuring the change in thermodynamic properties, such as heat capacity, or by dynamic mechanical thermal analysis (DMTA) measuring the change in the rheological properties, such as the storage and loss moduli. Of those measurement techniques, DSC has become the most popular. During a DSC measurement, the T_g determination should take into account the effect of intrinsic factors and extrinsic factors. In general, the intrinsic factors include the following: (i) sample composition, such as the presence of impurities, especially the universal plasticizer water, which depresses the sample's T_g greatly (**Table 3**); and (ii) thermal history, which determines the sample's physical states. For example, the presence of crystals due to recrystallization after the manufacture of an amorphous solid decreases its specific heat capacity over the glass transition range, and its melting peak during heating could overlap with the glass transition signals if it appears in the vicinity of T_g. Furthermore, the enthalpy recovery peak due to physical aging (**Figure 7**) could shift the glass transition temperature determined by the corresponding instrument software. As described by Wungtanagorn and Schmidt (*23*), the software-measured T_g of fructose and glucose glasses was shifted to higher temperature due to physical aging. In their studies, the physical aging of <7 days shifted the T_g midpoint by <5 °C. They suggested that the shift or increase of T_g measured by software was due to the increased overshoot and the shift of the overshoot peak, both of which were caused by the increased time of physical aging. However, theoretically, the calculated T_g (also called the fictive temperature T_f), determined from the intersection of the extrapolated glassy and liquid enthalpy curves, was expected to decrease with increased aging time due to a decrease in enthalpy as the sample approached equilibrium (**Figures 12** and **13**).

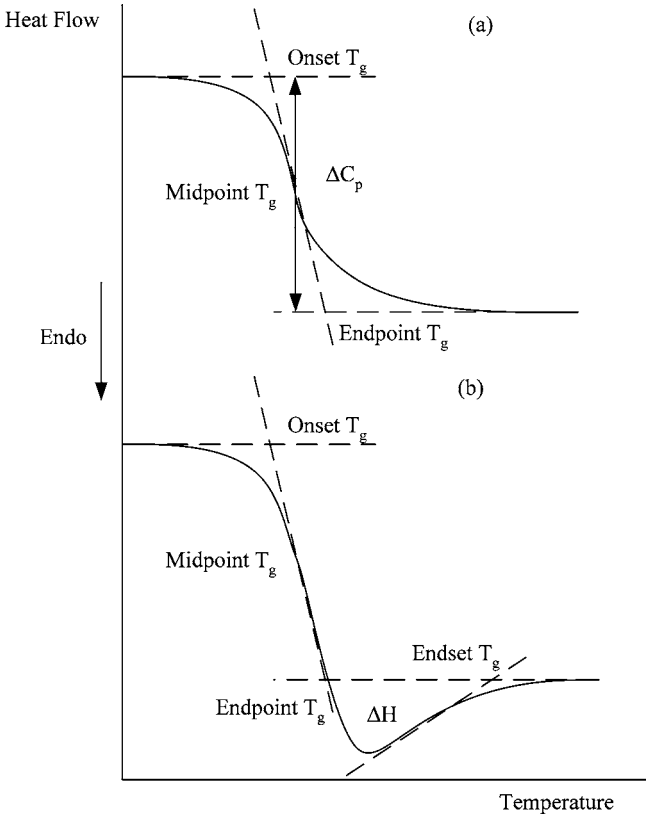

Figure 7. Glass transition measured using DSC for (**a**) an unaged sample showing the locations of the onset, midpoint, endpoint, and endset T_g values and change of heat capacity ΔC_p at T_g and (**b**) an aged sample where the area under the endotherm associated with T_g is defined as enthalpy recovery ΔH.

The extrinsic factors due to the kinetic character of glass transition include the following: (i) heating rate, on which the glass transition temperature's dependence is well-known (the higher the heating rate, the higher the T_g measured by DSC); (ii) cooling rate, if the glass sample is created by cooling from a melt, on which the glass transition temperature's dependence could be described as the higher the cooling rate, the higher the determined T_g, provided the scanning rate for T_g determination is the same; (iii) occurrence of glass transition over a temperature span (in general 5−20 °C for food saccharides), due to which it is hard to choose a single temperature to report as the sample's T_g, because none of the software-measured T_g values (onset, midpoint, end) has a clear physical meaning (**Figure 7**).

To make the DSC-determined T_g consistent and comparable for reported values in the literature, generally, the following recommendations are made:

(i) If the T_g of an anhydrous sample is desired, it is suggested to dry the sample in a vacuum oven at 60 °C under a pressure of <50 mmHg for 24 h before the analysis, or to equilibrate

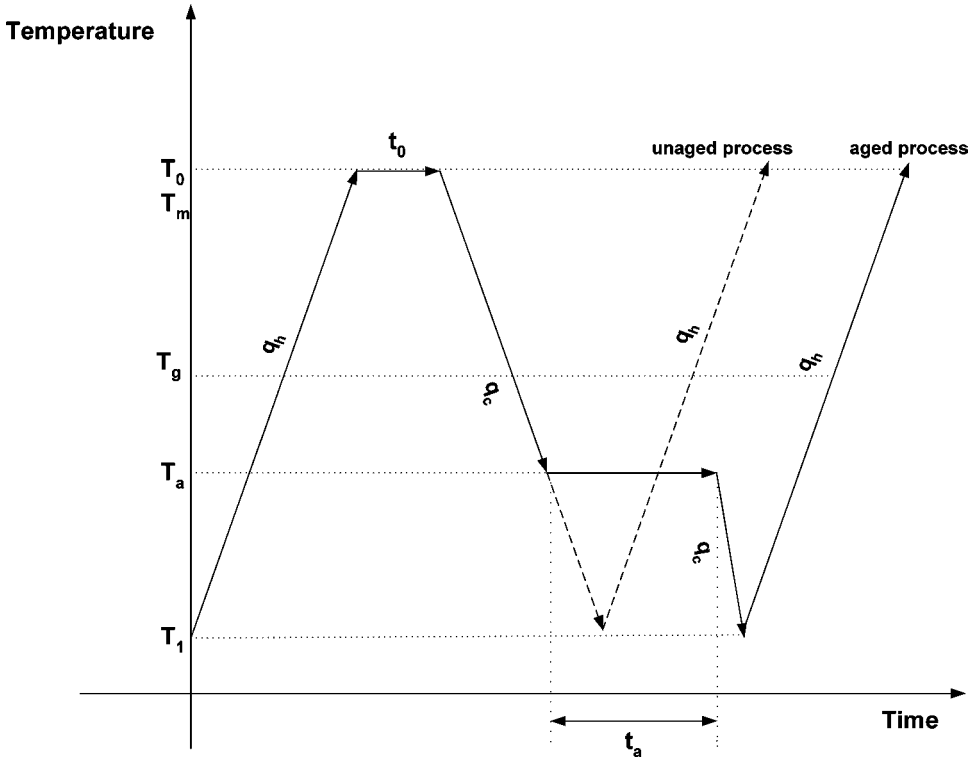

Figure 8. DSC temperature profile to create sugar glassy structure, determination of T_g of created glass, and measurement of the enthalpy relaxation of glass at aging temperature T_a for aging time t_a.

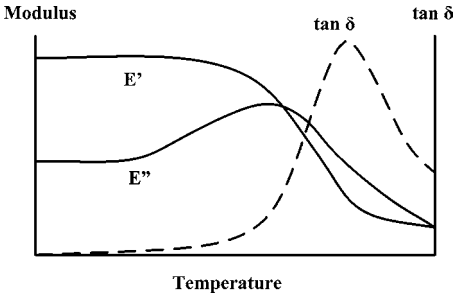

Figure 9. Glass transition measured by DMTA: α relaxation (adapted from ref *7*).

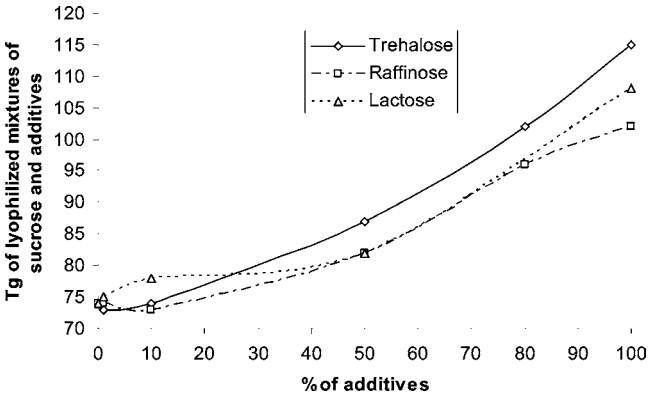

Figure 10. Glass transition temperature (midpoint) for various proportions of colyophilized mixtures of sucrose and additives (trehalose, raffinose, and lactose) (data obtained from ref *26*).

the sample in a desiccator above P_2O_5 desiccant at room temperature (25 °C) for 1 week, or to pierce a hole on the DSC pan lid and heat the sample to 120−130 °C to evaporate all water prior to the determination of T_g, provided chemical change is avoided during this process.

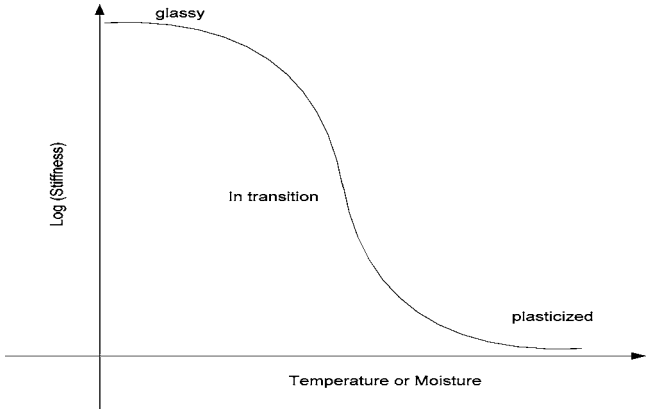

Figure 11. S-shape relationship between stiffness and moisture or temperature for food stored near T_g (modified from ref *53*).

(ii) If the T_g peak interferes with other peaks that are induced by its thermal history, such as enthalpy recovery due to aging or melting of recrystallized crystals, it is suggested to heat the sample to a temperature 40 °C above its glass transition temperature to erase its thermal history from the physical aging, or to heat the sample to a temperature above its melting temperature to remelt the formed crystals (**Figure 8**), or to use a temperature-modulated DSC (TMDSC) to separate the reversible transitions (glass transition, melting) and nonreversible transitions (enthalpy recovery and evaporation).

(iii) Due to the occurrence of glass transition over a temperature range, it is suggested to report at least two parameters, such as the onset or midpoint temperature and the transition width (*7*).

(iv) The experimental conditions should always be clearly reported together with the glass transition temperature, such as heating rate and cooling rate, and it is recommended to keep the heating rate at 10 °C/min in accordance with the material science convention, to make the heating rate equal to the cooling

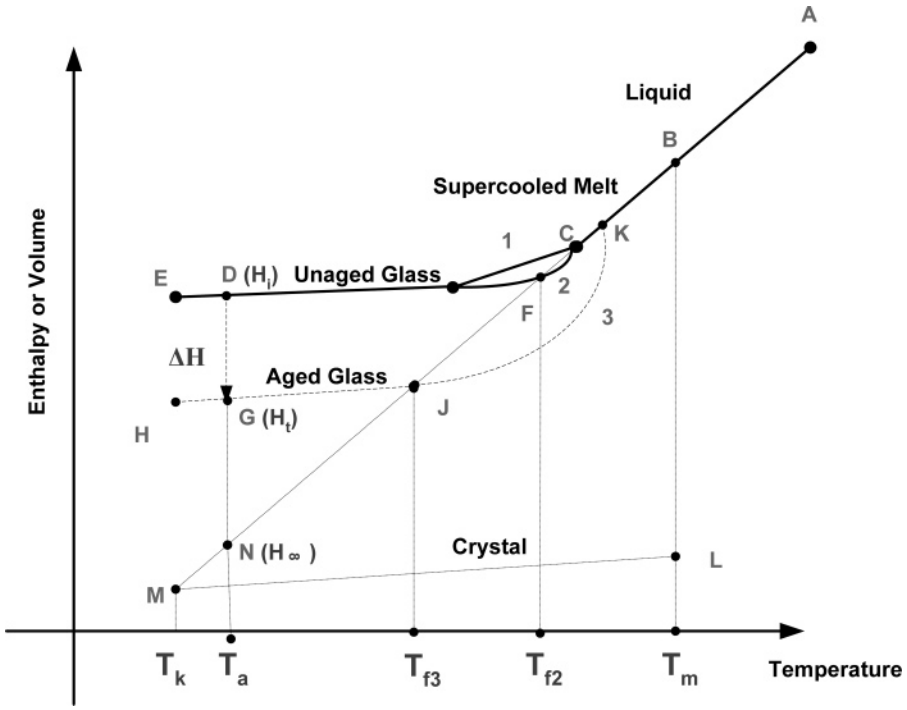

Figure 12. Schematic diagram of the change in enthalpy of a glass with isothermal aging and without aging.

rate when the glass is created by cooling from a melt, and to keep this experimental condition consistent through the whole study.

(v) If the effect of pressure on T_g shift is a concern, it is recommended to use a high-pressure DSC (HPDSC) to determine T_g. However, generally this is not a concern for food analysis, as food is usually stored and tested under atmospheric pressure. However, if during heating the evaporation of volatile components has a significant effect on the T_g determination, it is recommended to use HPDSC to suppress the evaporation.

Despite the recommendations described above, modification of DSC analysis should be made on the basis of the nature of the research and meet the research objectives. Generally, this requires the accumulation of research experience and in-depth understanding of the scientific issues involved.

Measurement of the glass transition temperature of food saccharides usually involves the melting of crystals and fast cooling of the melt to create a glass. The glass transition temperature is determined through reheating of the created sugar glass. A typical DSC temperature profile is shown in **Figure 8**.

However, among sachharides, when the lower molecular weight compounds such as sugars are heated at temperatures around their melting temperature, they change into brown materials called caramel. **Table 2** lists the peak melting temperature of some common sugars and their corresponding thermal degradation temperature at different heating rates. The thermal degradation temperature of most sugars is in the vicinity of their corresponding melting temperature at relatively slow heating rates ($\leq$10 °C/min). Only at the very fast heating rates ($\geq$20 °C/min) is the thermal degradation temperature higher than and not in the vicinity of their corresponding melting temperature. Therefore, during the melting of sugar crystals to create a sugar glass through DSC, the thermal degradation could be avoided only at the relatively fast heating rates. However, due to the limitation of some instruments, the fastest heating rate may be restricted. Therefore, the creation of glass through melting crystals and fast cooling needs to be carefully studied before it is applied. The impact of the melting conditions of sucrose crystals on the glass transition temperature of the sucrose melt was studied by Vanhal and Blond (*35*). Final temperature, heating rate, and residence time at the final temperature were the experimental conditions that affected the T_g measured. In their study, T_g decreased with increasing heating temperature, increasing residence time, and decreasing heating rate; that is, T_g decreased when the proportion of small molecules (glucose and fructose) increased due to the thermal degradation of sucrose. Howver, T_g increased after severe thermal treatment, that is, when the proportion of molecules with higher molecular weight (polymerization products) in the melt increased. In principle, the degradation should not occur prior to melting due to the stable structure and lack of molecular mobility in crystals. However, in some sugars such as sucrose and fructose, the degradation temperature is found even below the melting temperature (**Table 2**). This might be due to the degradation of residual amorphous solids remaining on the crystal surface during their manufacture. Normally, during the manufacture of crystal products, some liquid residue that is very viscous remains on the surface of the crystals. This residue does not crystallize due to either increased viscosity or the presence of a high amount of impurities that inhibit and/or interfere with the crystallization. During heating, this amorphous residue is changed to a supercooled melt, which has higher molecular mobility than the crystals at the same temperature. Therefore, it is more susceptible to thermal degradation, which may be well before the crystals melt and degrade.

As mentioned in section 2.2, there are heterogeneous amorphous structures in native starch, and this complex structure brings difficulties in the measurement of the T_g of starch. In native starch granules, amorphous regions distribute in different areas, where they interact differently with their neighborhood molecules. These interactions result in different molecular mobilities in the corresponding amorphous regions and thus different glass transition temperatures. Over the glass transition range, only starch molecules in the amorphous regions are involved in the state transition. Generally, this state transition in starch refers only to segments of the starch main chain and

not the whole long and complex main chain. Due to the interaction between crystalline and amorphous regions in starch and the resulting small changes in specific heat capacity through the glass transition range, the determination of starch T_g by DSC is difficult. A simplified "three-microphase" model has been proposed to describe the thermal behavior of granular starch (*15*). In this model, there are three types of microphase in starch: the rigid crystalline phase, the bulk and mobile amorphous phase, and the intercrystalline rigid−amorphous phase. Among the three phases, only the bulk and mobile amorphous phase contributes to the heat capacity change during the glass transition determined by DSC.

In the literature, it is a common practice to destroy the crystalline regions to convert them to amorphous before the determination of starch T_g. Generally, this could be done by gelatinization of starch granules with excessive water through heating. The starch paste is then dried with its moisture content adjusted to proper levels before the measurement. During the drying of the starch paste, retrogradation should be avoided or minimized as the recrystallized ordered regions may result in heterogeneity in amorphous regions again (*16*), but the T_g measured in this way is different from the T_g of the native starch. According to Chung et al. (*37*), there are several reasons why the T_g of native starch could be different from that of destroyed starch. First, the crystalline domains are surrounded by continuous amorphous regions in starch granules, and thus they behave like cross-linkages to the amorphous regions, suppressing the amorphous chain mobility. Second, intercrystalline amorphous phases, which may have a mixed structure between pure crystalline and amorphous structure, can exist in starch granules, and thus the amorphous transition is not clearly independent of crystalline melting. Third, there may be significant heterogeneity in the amorphous structure in native starch granules, possibly due to the mixed composition of amylose and amylopectin, both of which have a high polydispersity and are constituents of the amorphous regions.

Generally, for anhydrous amorphous starch, T_g is experimentally inaccessible, and its estimated T_g is in the range of 230−240 °C (*29*). During the heating of anhydrous amorphous starch, thermal degradation of starch polymers could take place before the T_g range. A common practice is to add water to the starch to bring down its T_g so that it could be determined before the thermal degradation takes place. Then the anhydrous starch T_g could be calculated on the basis of extrapolation or mathematical models of T_g.

Chung et al. (*37*) measured the T_g of native and gelatinized rice starches at various water contents using DSC. In low moisture content range (8-rela8%), the glass transition temperature of the native starch was higher (up to 20 °C) than that of the gelatinized starch, and the difference became greater as the moisture content decreased. The T_g of anhydrous starch could not be determined experimentally due to the thermal decomposition of the starch. On the basis of pure water's T_g (−139 °C) and ΔC_p (1.94 J/g·°C at T_g), the estimated T_g and ΔC_p of the anhydrous native rice starch were 296 °C and 0.285 J/g·°C, respectively, and those of the gelatinized rice starch were 180 °C and 0.500 J/g·°C, respectively. The T_g values were significantly different (>100 °C) between the native and gelatinized rice starches (*37*). In another study (*29*), the T_g of anhydrous starch was estimated to be 243 °C on the basis of the Fox and Flory equation.

Chung and Lim (*38*, *39*) and Chung et al. (*16*) studied the effects of aging temperature, aging time, and crystallinity on the glass transition and enthalpy relaxation of normal and waxy rice starch, including changes in the experimentally determined glass transition temperature, heat capacity, and maximum enthalpy relaxation. Together with the intrinsic factors of the rice starch, the experimental conditions may also play an important role in the results, as extensively discussed by Surana et al. (*40*) and Yu and Christie (*41*). Meanwhile, dual glass transitions were observed in normal rice starch, which suggests that the amorphous regions in the normal rice starch are heterogeneous (*16*).

Although the glass transition temperature is generally measured by DSC, for products containing starch and flour, DSC does not seem to be sensitive enough to detect the glass transition, due to the specific heat change during the glass transition being very small. Alternatively, DMTA could be used to determine the sharp change in the reheological properties through the glass transition so that the glass transition temperature could be measured. In DMTA, the glass transition temperature is presented as T_α (temperature with indication of measurement frequency). T_α could be determined from the temperature dependence of the storage modules (E') and loss modulus (E''), and it can be taken as the temperature at which E' starts to fall rapidly with increasing heating or the temperature at which E'' or the ratio of the loss modulus to the storage modulus (i.e., tan δ) reaches a maximum or the temperature at which E' and E'' coincide (**Figure 9**). However, the temperatures T_g and T_α should not be considered as fully equivalent, as explained by Champion et al. (*7*).

3.5. Models for the Prediction of the Glass Transition Temperature. The glass transition temperature is strongly dependent on molecular weight (*5*). Components that decrease the average molecular weight of a sugar mixture generally decrease the mixture's glass transition temperature (*42*). The following expression is used to describe the dependence of T_g on molecular weight in a homogeneous polymer series, such as saccharides containing glucose monomers

$$\frac{1}{T_g} = \frac{1}{T_{g\infty}} + \frac{K}{\mathrm{DP}} \tag{5}$$

where DP is the degree of polymerization, K is a constant, and $T_{g\infty}$ is the high molecular weight limit of T_g. According to this expression, the more glucose monomers the saccharide contains, the higher its T_g. For the data in **Table 1**, this rule is obeyed.

The Gordon−Taylor equation has been used to predict the T_g of a binary mixture

$$T_g = \frac{x_1 T_{g1} + K x_2 T_{g2}}{x_1 + K x_2} \tag{6}$$

where T_g, T_{g1}, and T_{g2} are the glass transition temperatures of the binary mixture, component 1, and component 2, respectively, x_1 and x_2 are the molar fraction or weight fraction of components 1 and 2, respectively, and K is the arithmetic average of a series of K values that are obtained by solving the equation for a series of binary systems at different ratios of components 1 and 2. The assumption of the Gordon−Taylor equation is ideal volume mixing, which assumes that the two components are miscible and their free volumes are additive (*43*). According to the free volume theory, K is related to the ratio of the free volumes of the two components (*44*) and can be calculated using the Simha−Boyer rule (*45*)

$$K \approx \frac{T_{g1}\rho_1}{T_{g2}\rho_2}$$

where ρ_1 and ρ_2 are the densities of components 1 and 2, respectively.

K can also be estimated as

$$K = \frac{\Delta C_{p2}}{\Delta C_{p1}}$$

where ΔC_p is the change in heat capacity of a component between its liquid-like and glassy states. This K value is developed on the basis of the classical thermodynamic theory and with an assumption that the entropy of mixing in an amorphous mixture is purely combinatorial. In this situation, the Gordon−Taylor equation could be rewritten as the Couchman−Karasz equation:

$$T_g = \frac{\Delta C_{p1} x_1 T_{g1} + \Delta C_{p2} x_2 T_{g2}}{\Delta C_{p1} x_1 + \Delta C_{p2} x_2} \quad (7)$$

Truong et al. (*46*) derived the Couchman−Karasz equation and applied it not only to binary systems but also to ternary, quaternary, and higher order systems.

Although the Gordon−Taylor equation is well accepted to predict the T_g of binary mixtures, the assumption of ideal mixing associated with the free volume theory is seldom achieved in practice. The ideal mixing assumes that the free volumes are additive and that no specific interaction takes place between the components during mixing. With the assumption of ideal mixing, the low molecular weight compounds (plasticizer) have the plasticization effect (i.e., lower the value of T_g) as they have higher free volume than polymers, according to the free volume theory. The addition of plasticizers increases the free volume for polymers' molecular mobility. However, due to the presence of hydrophilic groups in the saccharides, their mixing usually induces the formation of hydrogen bonding, causing the mixture's T_g to be higher than the predicted value. However, the general trends are obeyed when saccharides are mixed; for example, athe ddition of mono- or disaccharides into polysaccharides lowers the T_g value. Kalichevsky et al. (*21*) studied the plasticization effect of sugars on amylopectin. They found the degree of plasticization appeared to increase in the following order: sucrose < glucose < xylose < fructose. Sucrose (T_g = 69 °C) is a disaccharide and has a higher molecular weight and T_g than the rest; therefore, it is expected to have a reduced plasticizing effect when compared to the other sugars. Glucose (T_g = 38 °C) and fructose (T_g = 7 °C) have the same molecular weight, but fructose has a lower T_g; therefore, fructose is expected to have a greater plasticizing effect. Xylose (T_g = 13 °C) has the lowest molecular weight but a slightly higher T_g than fructose.

It is also reported that the addition of small amounts of plasticizers or antiplasticizers has no significant effect on T_g. This is different from the prediction of the Gordon−Taylor equation. In the study of Shamblin et al. (*43*, *47*), small amounts (up to 25% w/w) of polymeric additives, such as Ficoll (T_g = 132 °C) or poly(vinylpyrrolidone) (PVP, T_g = 178 °C), had no significant effect on T_g of co-lyophilized sucrose (T_g = 74 °C), and the T_g values of various mixtures generally were lower than the values predicted by the Gordon−Taylor equation and the free volume theory. The reason is nonideal mixing due to the hydrogen bonds formed between the components in the lyophilized mixtures. In another study, up to 10% w/w addition of polysaccharides (linear polysaccrides such as dextran and pullulan, branched polysaccharides such as gum arabic) did not have any significant effect on the change in glass transition temperature of the maximal cryoconcentrated phase (T_g') of 58.5% w/w sucrose solution (*48*), and addition of corn syrup with various DEs up to 50% (w/w) did not have a significant effect on T_g of co-lyophilized mixtures with sucrose (*49*). In the study of Saleki-Gerhardt and Zografi (*26*), mixing of amorphous sucrose with different higher T_g amorphous additives, such as trehalose, raffinose, and lactose, showed similar trends at low amount of addition of the additives (**Figure 10**). Kets et al. (*50*) discovered that hydrogen bonding due to nondeal mixing could result in the mixture having a T_g higher than that of both individual components. The addition of low molecular weight sodium citrate into the high molecular weight sucrose is expected to lower the glass transition temperature. However, in their study, the T_g of the mixture of citrate and sucrose (up to 105 °C) was higher than the individual T_g values of both pure citrate and sucrose. Using FT-IR, the rise of the T_g of the mixture was found to be due to the strong hydrogen bonding between citrate's carboxylate groups and sucrose's OH groups.

In food systems, water is the major component acting as a plasticizer, and its theoretical glass transition temperature is −137 °C (136 K). The T_g value of a given hydrophilic substance is decreased with an increase in water content, following a nonlinear function as described by the Gordon−Taylor equation. The plasticization effect of water on the glass transition of lyophilized sucrose is shown in **Table 3**.

However, the effects of water on molecular mobility including plasticization are poorly understood mainly because molecular and structural analyses are scarce. Kilbrun et al. (*51*) concluded that the plasticization effect of water in carbohydrates is via a complex mechanism involving both hydrogen bond formation and disruption and changes in the matrix free volume. In the dry state, the hydrogen bonding between carbohydrate molecules leads to the formation of large molecular entities. When water is absorbed, it disrupts the hydrogen bonds between the carbohydrate chains. Two effects of absorbed water on a glass were proposed. First, water tends to fill the smallest voids in the glassy matrix. Second, the absorbed water, due to its interference with the intermolecular hydrogen bonding of the carbohydrates, increases the degree of freedom of the carbohydrate chains, leading to a "cold" relaxation of the chains and coalescence of the smallest voids under the driving force associated with the reduction of free surface area (i.e., the surface tension).

Besides water, small molecules such as sugars have also been found to act as plasticizers in biopolymer systems, increasing the free volume (or the defect concentration) between the molecules, provided there is no phase separation (*7*). Branching in polysaccharides may work as an internal plasticizer, inducing a small decrease in T_g when compared to linear chains (*52*).

3.6. Influence of Glass Transition on Food Stability. Food stability depends on the mobility on a molecular basis, which determines physical and chemical changes and the resulting quality. In liquids, the translational or rotational diffusion of molecules is a possible reactant in an alteration reaction. These diffusions can be predicted according to the Debye−Stokes−Einstein (DSE) relationships

$$D_{trans} = \frac{k_B T}{6\pi\eta r c}$$

$$D_{rotat} = \frac{k_B T}{8\pi\eta r^3 c}$$

where T is the absolute temperature, k_B is the Boltzmann

constant, η is the viscosity, r is the hydrodynamic radius of the diffusant, and c is the coupling factor between the molecules and the matrix.

However, the DSE equations could not be used to describe the diffusion of a small solute dispersed in a polymer network, where the macroscopic viscosity (commonly measured) does not reflect the local diffusion condition, for example, in glass. In the vicinity of T_g, the translational diffusivity may be 2−5 orders of magnitude higher than that predicted from the viscosity and the DSE equations, due to the facilitation by local motion of the matrix (*5*). The influence of T_g on the translational diffusivity or the diffusion of molecules has an important impact on the diffusion-controlled physical and chemical processes, which limit the shelf life of food products. Thus, the stability of food products may be dependent on the position of storage temperature versus T_g (*12*). Peleg (*53*) proposed an S-shape relationship between stiffness or brittleness and moisture or temperature (**Figure 11**). In its idealized form it can be described by the mathematical expression

$$Y(X) = Y_s \cdot \frac{1}{1 + \exp\left(\frac{X - X_c}{a}\right)}$$

where X is temperature, moisture, or water activity, $Y(X)$ is the magnitude of the corresponding mechanical parameter, Y_s is the value of $Y(X)$ under the glassy state at a reference condition ($X \ll X_c$), if it can be assumed to be constant, X_c is a critical level of X signifying the inflection point of $Y(X)$, and a is a constant that represents the steepness of the relationship around X_c.

The concept of glassy/rubbery states was mainly used to interpret the stability of low-moisture foods and biomaterials, which have been extensively discussed by Le Meste et al. (*5*), Champion et al. (*7*), Rahman (*6*), and others. Currently, the glass transition concept has been linked to microstability, chemical stability, and especially physical stability, such as structure, texture, collapse, caking, drying, extrusion, and crystallization. Meanwhile, certain food processing and preservation methods, such as encapsulation and edible film, have also been linked with glass transition (*5*).

4. ENTHALPY RELAXATION

The only thermodynamic equilibrium state below the melting point is the crystalline state. Glass is in a nonequilibrium state. When a glass is stored below its glass transition temperature, it will spontaneously approach the more stable state, due to its nonequilibrium nature. This kind of change is called enthalpy relaxation or structural relaxation or physical aging. Glass always recognizes the presence of a more stable glassy state and continuously evolves toward it in a manner predictable from its thermal history and the degree of nonequilibrium (*9*).

In a glass, the translational and rotational mobilities of large molecules are restricted. Only the local vibration and reorientation of small groups of atoms still exist (*5*), and those motions do not involve the surrounding atoms and molecules and are mainly local. In the glass transition temperature zone, molecular mobility is mainly presented as the primary α relaxation, which is the glass to liquid transition. Below the glass transition temperature, the secondary relaxations are observed, namely, β and γ relaxations as temperature decreases. Different from α relaxation, β relaxation is caused by the motion of specific chemical groups such as the side groups branched on a polymer chain. In other words, β relaxation is the motion of a short sequence of the molecules ("crankshaft motion") in regions where density and intermolecular forces are at minimum. For example, β relaxation could occur as a result of the internal rotation of the main chain of a polymer toward reducing the configurational energy, according to the chemical structure and hydrogen bonding formation (*53*). The secondary relaxation is considered to be a continuation of the primary relaxation (*5*). Simply speaking, α relaxation is general, cooperative, non-Arrhenius, linked to viscous flow, and synonymous with the glass transition, but β relaxation is specific, local, Arrhenius, and of molecular origin (*9*). Similar to β relaxation, γ relaxation, which takes place at lower temperature than β relaxation, is also localized and non-co-operative, but compared to β relaxation, γ relaxation is much weaker (*54*).

Several sub-T_g relaxations can be observed in biopolymers and low molecular weight sugars (β and γ relaxations). Their origin is still being discussed (*5*). As observed in polysaccharides (*10*), they could correspond to the rotation of lateral groups (γ relaxation at low temperature) or local conformation changes of the main chain (β relaxation close to T_g). The apparent activation energy ranges between 40 and 70 kJ/mol for β relaxation in maltose and glucose (*55*) and between 5 and 19 kJ/mol for γ relaxation in ethyl cellulose (*10*). When a glass is stored between T_β (β relaxation temperature) and T_g, usually 20−40 K below T_g, a microstructure evolution may take place, which corresponds to the system approaching a metastable equilibrium, with some extra loss in its enthalpy and volume.

Measurement of the enthalpy relaxation is commonly carried out with a glass in which all thermal treatment histories have been erased. This can be done by heating an amorphous solid to a temperature at least 40 K greater than T_g (*27*) or by melting a crystalline material and then cooling it to the amorphous phase at a suitable cooling rate. However, during this process, thermal decomposition needs to be avoided. The sample then goes through aging if necessary. The enthalpy relaxation can be measured by reheating the sample. **Figure 12** illustrates this process.

In **Figure 12**, paths ABCDE and EDFCBA represent the cooling and reheating processes, respectively. Path DG represents an isothermal aging process, and path HGJKBA represents the reheating process after the aging, during which an endothermic overshoot is observed in the glass transition region. This overshoot near T_g during reheating is due to a rapid recovery of the lost enthalpy or the extra entropy through the aging, and it could be used to measure the lost enthalpy during the aging process by DSC. In **Figure 12**, the sample is cooled at a cooling rate q_c and heated at a heating rate q_h. H_i and H_t are the enthalpies at the beginning of an aging and at time t of the aging, respectively. The equilibrium enthalpy at aging temperature T_a is assumed to be H_∞, which is represented as point N on the extrapolated equilibrium liquid curve at the aging temperature T_a. C_{pl} is the specific heat of the equilibrium liquid, and C_{pg} is that of the glass. The following equations could be derived:

$$\Delta H = H_i - H_t$$

$$\delta_H = H_i - H_\infty = (C_{pl} - C_{pg})(T_g - T_a)$$

In **Figure 12**, T_{f2} and T_{f3} are fictive temperatures of the unaged and aged samples, respectively. Fictive temperature is a hypothetical temperature at which the structure of the glass would be in equilibrium (*62*). Fictive temperature is a function of the sample temperature. At a sample temperature well below the transition region, it is equivalent to the intersection point of

the enthalpy curves for the glassy state and the equilibrium liquid state (**Figure 12**) and named the limiting fictive temperature (T_f). The limiting fictive temperature, normally called the fictive temperature, can be calculated by solving the equation (*57*)

$$\int_{T_2}^{T_f} (C_{pl} - C_{pg})\, dT = \int_{T_2}^{T_1} (C_{pt} - C_{pg})\, dT$$

where C_{pl}, C_{pg}, and C_{pt} are the specific heat of the material at the liquid state, glass state, and transition region, respectively. T_1 is a temperature well below the transition region, and T_2 is a temperature above the transition region. According to Montserrat (*58*), the fictive temperature could be estimated as

$$T_f(T_a,t_a) \approx T_g - \frac{\Delta H}{\Delta C_p}$$

where T_g and ΔC_p are from unaged sample and ΔH is the relaxed enthalpy through aging.

The dependence of the glass transition temperature determination on experimental conditions such as heating and cooling rates has been discussed under section 3.4, and it is well described in the literature. Recent research has found that the enthalpy recovery at T_g determined by DSC is also dependent on experimental conditions, including heating rate and the combination of heating and cooling rates (*40*). For the same sample aged at the same temperature for the same duration, the higher the heating rate, the larger the value of enthalpy recovery determined by DSC, and the difference between those brought by higher heating rate and lower heating rate increases with aging time. When samples with identical thermal histories are heated, a lower heating rate would usually allow a sample to stay longer below its T_g during heating, therefore relaxing more. If this is the case, higher heating rates should result in lower enthalpy recovery. In fact, experimental results suggest the opposite (*40*). With higher heating rate, the onset and endset of glass transition (**Figure 7b**) are all shifted to higher temperatures, and the width of the enthalpy recovery (distance between the onset and endset temperatures) is increased as well. The elevated onset T_g results in a wider transition range for enthalpy recovery to reach the equilibrium rubber state at higher temperature (endset T_g). This results in more enthalpy recovery (*40*), and this effect is amplified with increased aging time. The effect of heating rate on enthalpy recovery determination is clearly illustrated in **Figure 13**. Besides the heating rate, the ratio of cooling rate to heating rate also has an impact on the enthalpy recovery determination. In general, with an increase in the ratio of heating rate to cooling rate, there is an increase in the determined enthalpy recovery for the same sample, and this effect is minimized with equal heating and cooling rates (*40*). To minimize the impact of experimental conditions on the enthalpy relaxation determination, we suggest that a medium heating rate (10 °C/min) and an equal cooling rate be used for enthalpy relaxation studies. However, most researchers prefer to use a higher cooling rate to create a glass (with higher T_g) from a rubber. In such situations, the experimental conditions must be kept the same during the whole study so that their impact is kept consistent. In this respect, the enthalpy relaxation studies done by various researchers using different experimental parameters may not be comparable to each other. This brings difficulties to the analysis of the current literature results, such as those in **Table 4**. This may also explain why the literature values from different researchers vary from one another. However, to our knowledge, so far the study of Surana et al. (*40*) is the only one that addressed the effect of experimental conditions on the determined enthalpy recovery by DSC. This area requires more research to confirm the findings.

In general, the enthalpy relaxation of amorphous materials is accompanied by changes in macroscopic properties, such as density, mechanical strength, and transport properties (*58*). In the field of synthetic polymers, the enthalpy relaxation is recognized as an important factor for changes in the physical properties of polymers, because the rate of the enthalpy relaxation is estimated as the molecular motion at temperatures below T_g (*54*). The enthalpy relaxation is both nonexponential and nonlinear (*5*). Several models involving the relaxation time τ can be used to describe the characteristics of the enthalpy relaxation.

4.1. Nonexponentiality. The enthalpy relaxation process cannot be described by a simple relaxation function, due to the microstructural heterogeneities of the materials that have been discussed in the previous section. However, it can be described by a so-called stretched exponential relaxation function, known as the Kohlrausch−Williams−Watts (KWW) expression

$$\Phi(t) = \exp\left[-\left(\frac{t}{\tau}\right)^{\beta}\right] \quad (8)$$

where $\Phi(t)$ is the property of concern, which is a function of time t. For example, in the enthalpy relaxation study using DSC, $\Phi(t)$ is the portion of unreleased enthalpy using the metastable equilibrium state at the aging temperature as the reference state, that is

$$\Phi(t) = 1 - \frac{\Delta H}{\delta_H}$$

τ is the mean molecular relaxation time, and β is a constant characterizing the width of the relaxation time distribution spectrum ($0 \le \beta \le 1$); $\beta = 1$ corresponds to a single relaxation time with exponential behavior. The smaller the value of β, the more the distribution of molecular motion deviates from a single-exponential behavior. In other words, if β is significantly different from 1, it indicates a distribution of relaxation time rather than a single relaxation time. The parameter β has been shown to correspond to the strength/fragility of a material above T_g. It is close to 1 for strong liquids (nearly exponential relaxation) (*5*). For fragile liquids, β changes from near 1 at high temperatures to a value close to 0.3−0.5 near the T_g (*5*), but no similar relationship has yet been established below T_g (*1*). It was reported that small molecules had higher β values than polymers. For example, the β values for starch (0.23−0.34) in the paper by Kim et al. (*8*) were smaller than the β values calculated for sucrose (0.4−0.8) (*59*). In other studies (*24*, *27*), the β values for sucrose, glucose, and fructose were 0.33, 0.64, and 0.50, respectively.

4.2. Nonlinearity. The characteristic relaxation value τ changes with time, as it depends on both temperature and the average structural state of the glass that depends on its previous thermal history. This nonlinear character of the enthalpy relaxation is commonly described by the following Tool−Narayanaswamy−Moynihan (TNM) expression

$$\tau = \tau_0 \exp\left(\frac{x\Delta h}{RT_a} + \frac{(1-x)\Delta h}{RT_f}\right) \quad (9)$$

where τ_0 is the relaxation time in equilibrium at an infinitely high temperature, Δh is the apparent activation energy (a constant) in the equilibrium state above T_g, and R is the ideal gas constant. The fictive temperature T_f, for a material at the

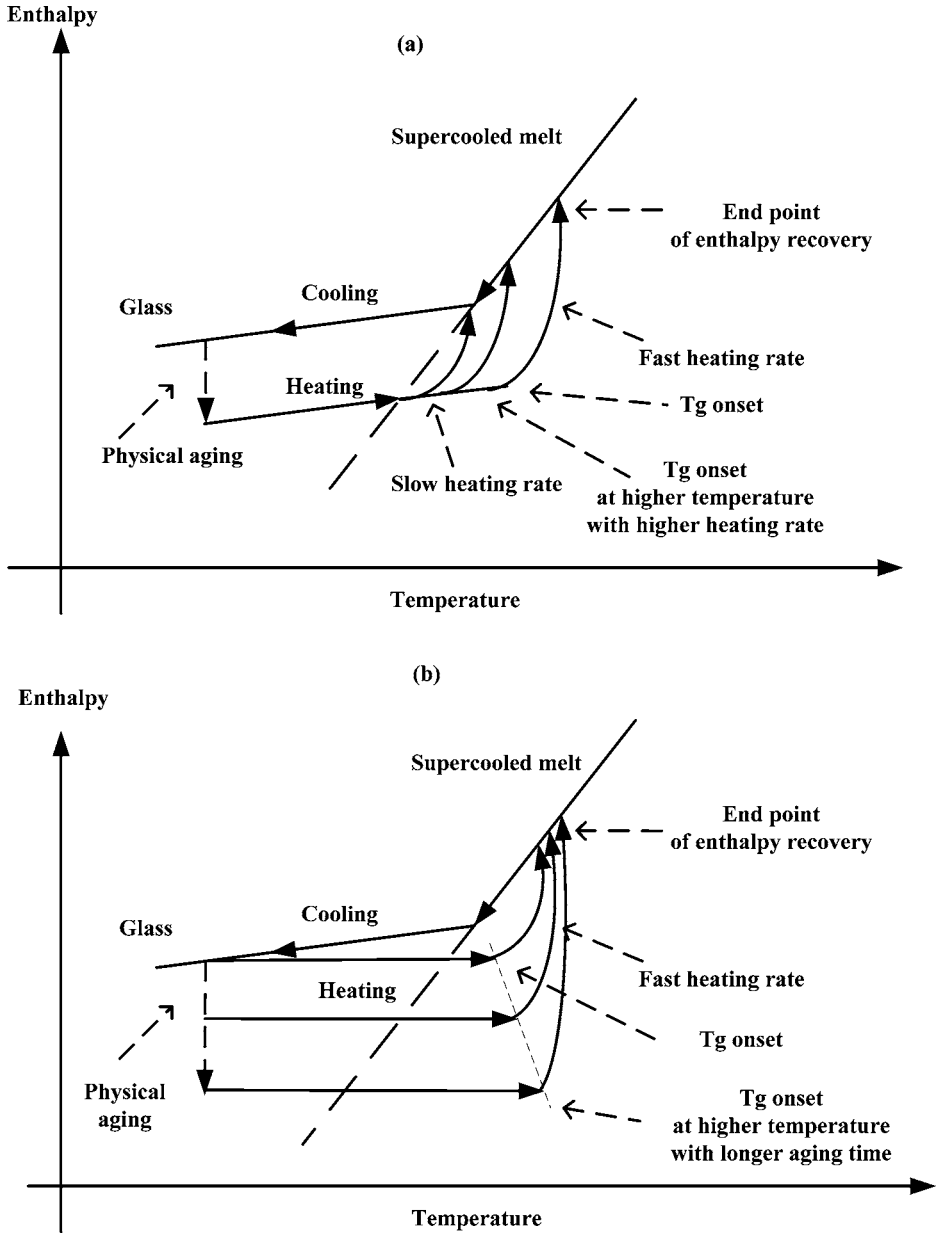

Figure 13. Schematic representation of the predicted thermodynamic behavior of an aged amorphous substance: (**a**) constant aging time followed by heating at different rates; (**b**) changing aging time with constant heating rate (adapted from ref *40*).

actual temperature T, is considered to represent its structural state. T_a is the aging temperature. The parameter x ($0 \leq x \leq 1$) defines the relative contributions of temperature and structure to τ. If x is close to 1, τ mainly depends on the aging temperature. The parameters τ, β, and x can be estimated from enthalpy relaxation experiments using DSC after varation of the annealing times (*60*). In the literature, addition of fructose to a glucose−fructose system increases the x value and increases the linearity of relaxation (*24*).

The strong/fragile classification can also be used to describe the temperature dependence of the relaxation properties in the equilibrium state. Fragility indicates how quickly the structural relaxation accelerates as a glass approaches and traverses the glass transition region (*9*). Fragile liquids have strong temperature dependence of viscosity and molecular mobility; thus, they exhibit larger changes of relaxation time in the vicinity of the glass transition than strong liquids. The glass transition temperature T_g has also been related with the structural relaxation. For example, the addition of some additives, such as antiplasticizers or additives with higher T_g, can reduce the molecular mobility and increase the T_g. The rate of the enthalpy relaxation is decreased, as expected, upon the addition of a substance with higher T_g, for instance, dextran in sucrose (*43*). In contrast, increasing the weight fraction of fructose in glucose−fructose mixtures also results in a decrease of the aging rate, although T_g is depressed (*24*).

Currently, little information has been reported on the kinetic data of the enthalpy relaxation process of food saccharides (**Table 4**), which may be a useful tool for predicting the changes in physical properties during storage. According to Kim et al. (*8*), the value of τ for starch increased with decreasing aging temperature, in the same manner as that for sucrose, indicating that the aging process is slower at lower T_a. This is because the motion of relaxed molecules or segments of polymers becomes more restricted with increasing distance from T_g. Compared to the data for sucrose, the τ value of starch was slightly larger, which suggests that the starch is more stable than sucrose at the same temperature range. This may be due to its high molecular weight and structure complexity such as branching. The entanglement effect of polymers may also contribute to

Table 4. Kinetic Data of Enthalpy Relaxation of Selected Food Saccharides

sample	T_g (°C)	$T_g - T_a$ (°C)	β	τ (h)	δ_H (J/g)	ref
sucrose	77	16	0.2–0.8	300[a]		59
		32		20000[a]		
		47		3000000[a]		
	68.5	8.5	0.32			27
		13.5	0.32			
		23.5	0.32			
	78	17			10.9	28
maltose	41	11	0.41	2.27	7.02	25
	37.36[b]	14.4[b]	0.44[b]	11.02[b]	7.33[b]	61
		24.4[b]	0.32[b]	1350.65[b]	13.33[b]	
	33.16[c]	13.2[c]	0.28[c]	20.90[c]	10.55[c]	
		13.2[c]	0.21[c]	4759.55[c]	16.55[c]	
fructose	16	11	0.515	1.66	4.795	62
	7	8.78	0.48	14.27	6.6	23
	5	10	0.505			22
glucose	38	9.89	0.56	3.35	7.14	23
	37	10	0.643			24
gelatinized potato starch (16% moisture)	59	34	0.34	312000		22
		26	0.23	15100		
		17	0.3	637		
gelatinized rice starch (14.5% moisture)	56.7 and 71.4[d]	$T_a = 25$ °C	0.336	624	2.064	38
gelatinized waxy rice starch (14.5% moisture)	70.7	45.7	0.401	316.8	1/764	38

[a] Estimated from curves. [b] Measured by standard DSC. [c] Measured by modulated DSC. [d] Dual glass transitions were detected due to heterogeneity of rice starch.

the slower aging process. The apparent Arrhenius activation energy (E_a) of gelatinized potato starch by using τ values is 284 kJ/mol (*8*). For sucrose, Hancock et al. (*59*) reported $E_a = 360$ kJ/mol.

When the variability of physical properties is considered, the concept of enthalpy relaxation is also important. Experimental results on the water vapor permeability of a starch film by Kim et al. (*8*) indicated that even under storage below the glass transition temperature, changes in the physical properties of the glassy starch could not be prevented as the enthalpy relaxation proceeded. The enthalpy relaxation or the secondary relaxations below the glass transition temperature are considered to be the continuation of the primary relaxation or glass transition. Enthalpy relaxation results from the local molecular motions of certain molecules or certain parts of polymer molecules, although its exact origins in complex food systems are hard to define. All food qualities, either chemical or physical, are related to the molecular mobility. Therefore, the enthalpy relaxation needs to be taken into consideration when quality is of a concern for foods stored below their glass transition temperature, which is common in food storage. Although currently very few studies have been reported on the relationship between the enthalpy relaxation and food quality, the enthalpy relaxation is believed to be as important as the glass transition to the quality of food stored below its glass transition temperature.

5. CONCLUSION

Through processing, many foods exist in the amorphous state, the stability of which is related to two important state transitions, glass transition and enthalpy relaxation. The glass transition temperature has been shown to be an effective indicator of food storage stability. However, there is evidence that localized molecular mobility continues even below the glass transition temperature, which results in the enthalpy relaxation of amorphous foods. Due to limited information on the enthalpy relaxation kinetics of food materials, its relationship to food stability is largely unexplored. This review emphasizes the importance of the enthalpy relaxation to food stability during storage. Generally, food should be stored at a temperature far enough below its glass transition temperature to largely retard the enthalpy relaxation.

ACKNOWLEDGMENT

We thank Dr. David Young for reading the draft manuscript and suggestions.

LITERATURE CITED

(1) Hancock, B. C.; Zografi, G. Characteristics and significance of the amorphous state in pharmaceutical system. *J. Pharm. Sci.* **1997**, *86* (1), 1−12.

(2) Bhandari, B. R.; Hartel, R. W. Phase transitions during food powder production and powder stability. In *Encapsulated and Powdered Foods*; Onwulata, C., Ed.; Taylor and Francis: New York, 2005; pp 261−291.

(3) Bhandari, B. R.; Howes, T. Implication of glass transition for the drying and stability of dried foods. *J. Food Eng.* **1999**, *40*, 71−79.

(4) Kim, Y. J.; Suzuki, T.; Hagowara, T.; Yamaji, I.; Takai, R. Enthalpy relaxation and glass to rubber transition of amorphous potato starch formed by ball-milling. *Carbohydr. Polym.* **2001**, *46*, 1−6.

(5) Le Meste, M.; Champion, D.; Roudaut, G.; Blond, G.; Simatos, D. Glass transition and food technology: a critical appraisal. *J. Food Sci.* **2002**, *67* (7), 2444−2458.

(6) Rahman, M. S. Glass transition and other structural changes in foods. In *Handbook of Food Preservation*; Rahman, M. S., Ed.; Dekker: New York, 1999; pp 75−93.

(7) Champion, D.; Le Meste, M.; Simatos, D. Towards an improved understanding of glass transition and relaxations in foods: molecular mobility in the glass transition range. *Trends Food Sci. Technol.* **2000**, *11*, 41−55.

(8) Kim, Y. J.; Hagiwara, T.; Kawi, K.; Suzuki, T.; Takai, R. Kinetic process of enthalpy relaxation of glassy starch and effect of physical aging upon its water permeability property. *Carbohydr. Polym.* **2003**, *53*, 289−296.

(9) Yu, L. Amorphous pharmaceutical solids: preparation, characterization, and stabilization. *Adv. Drug Delivery Rev.* **2001**, *48*, 27−42.

(10) Bidault, O.; Assifaoui, A.; Champion, D.; Le Mester, M. Dielectric spectroscopy measurements of the sub-T_g relaxations in amorphous ethyl cellulose: a relaxation magnitude study. *J. Non-Cryst. Solids* **2005**, *351*, 1167−1178.

(11) Perez, J. Theories of liquid-glass transition. In *Water in Foods*; Fito, P., Mulet, A., McKenna, B., Eds.; Elsevier Applied Science: New York, 1994; pp 89−114.

(12) Simatos, D.; Blond, G.; Perez, J. Basic physical aspects of glass transition. In *Food Preservations by Moisture Control: Fundamentals and Applications*; Barbosa-Canovas, Q. V., Welti-Chanes, J., Eds.; Technomic Publishing: Lancaster, PA, 1995; pp 1−31.

(13) Johari, G. P.; Goldstein, M. Viscous liquids and the glass transition II. Secondary relaxation in glasses of rigid molecules. *J. Chem. Phys.* **1970**, *53*, 2372−2388.

(14) Johari, G. P. Effects of annealing on secondary relaxations in glasses. *J. Chem. Phys.* **1982**, *77*, 4619−4626.

(15) Biliaderis, C. G. Structures and phase transitions of starch polymers. In *Polysaccharide Association Structures in Food*; Walter, R. H., Ed.; Dekker: New York, 1998; pp 57−168.

(16) Chung, H. J.; Lim, S. T. Physical aging of glassy normal and waxy rice starches: thermal and mechanical characterization. *Carbohydr. Polym.* **2004**, *57*, 15−21.

(17) Fennema, O. R. Water and ice. In *Food Chemistry*, 3rd ed.; Fennema, O. R., Ed.; Dekker: New York, 1996; pp 17−94.

(18) Broadhead, J.; Rouan Edmond, S. K.; Rhodes, C. T. The spray drying of pharmaceuticals. *Drug Dev. Ind. Pharm.* **1992**, *18*, 1169−1206.

(19) Chung, H. J.; Chang, H. I.; Lim, S. T. Physical aging of galssy normal and waxy rice starches: effect of crystallinity on glass transition and enthalpy relaxation. *Carbohydr. Polym.* **2004**, *58*, 101−107.

(20) Schmidt, S. J. Water and solids mobility in foods. *Adv. Food Nutr. Res.* **2004**, *48*, 1−101.

(21) Kalichevsky, M. T.; Jaroszkiewicz, E. M.; Blanshard, J. M. V. A study of the glass transition of amylopectin−sugar mixture. *Polymer* **1992**, *34* (2), 346−358.

(22) Orford, P. D.; Parket, R.; Ring, S. G. Aspects of the glass transition behavior of mixtures of carbohydrates of low macular weight. *Carbohydr. Res.* **1990**, *196*, 11−18.

(23) Wungtanagorn, R.; Schmidt, S. J. Thermodynamic properties and kinetics of the physcial ageing of amorphous glucose, fructose, and their mixture. *J. Therm. Anal. Calorim.* **2001**, *65*, 9−35.

(24) Wungtanagorn, R.; Schmidt, S. J. Phenomenological study enthalpy relaxation of amorphous glucose, fructose, and their mixture. *Thermochim. Acta* **2001**, *369*, 95−116.

(25) Schmidt, S. J.; Lammer, A. M. Physical ageing of maltose glasses. *J. Food Sci.* **1996**, *61* (5), 870−875.

(26) Saleki-Gerhardt, A.; Zografi, G. Non-isothermal and isothermal crystallization of sucrose from the amorphous state. *Pharm. Res.* **1994**, *11* (8), 1166−1173.

(27) Urbani, R.; Sussich, F.; Prejac, S.; Casaro, A. Enthalpy relaxation and glass transition behavior of sucrose by static and dynamic DSC. *Thermochim. Acta* **1997**, *304/305*, 359−367.

(28) Shamblin, S. L.; Zografi, G. Enthalpy relaxation in binary amorphous mixtures containing sucrose. *Pharm. Res.* **1998**, *15* (12), 1828−1834.

(29) Roos, Y.; Karel, M. Water and molecular weight effects on glass transitions in amorphous carbohydrates and carbohydrate solutions. *J. Food Sci.* **1991**, *56* (6), 1676−1681.

(30) Genin, N.; Rene, F. Analyse du role de las transition vitreause dans les procedes de conservation agro-alimentarie. *J. Food Eng.* **1995**, *26*, 391−407.

(31) Williams, M. L.; Landel, R. F.; Ferry, J. D. The temperature dependence of relaxation mechanisms in amorphous polymers and other glass-forming liquids. *J. Am. Chem. Soc.* **1955**, *77*, 3701−3707.

(32) Angell, C. A.; Bressel, R. D.; Green, J. L.; Kanno, H.; Oduni, M.; Sarre, E. J. Liquid fragility and glass transition in water and aqueous solutions. In *Water in Foods*; Fito, P., Mulet, A., McKenna, B., Eds.; Elsevier Applied Science: New York, 1994; pp 115−142.

(33) Angell, C. A. Formation of glasses from liquid and biopolymers. *Science* **1995**, *267*, 1924−1935.

(34) Crowly, K. J.; Zografi, G. The use of thermal methods for predicting glass-former fragility. *Thermochim. Acta* **2001**, *380*, 79−83.

(35) Vanhal, I.; Blond, G. Impact of melting conditions of sucrose on its glass transition temperature. *J. Agric. Food Chem.* **1999**, *47*, 4285−4290.

(36) Hurtta, M.; Pitkanen, I.; Knuutinen, J. Melting behavior of D-sucrose, D-glucose, and D-fructose. *Carbohydr. Res.* **2004**, *339*, 2267−2273.

(37) Chung, H. J.; Lee, E. J.; Lim, S. T. Comparison in glass transition and enthalpy relaxation between native and gelatinized rice starches. *Carbohydr. Polym.* **2002**, *48*, 287−298.

(38) Chung, H. J.; Lim, S. T. Physical aging of glassy normal and waxy rice starches: effect of aging temperature on glass transition and enthalpy relaxation. *Carbohydr. Polym.* **2003**, *53*, 205−211.

(39) Chung, H. J.; Lim, S. T. Physical aging of glassy normal and waxy rich starches: effect of aging time on glass transition and enthalpy relaxation. *Food Hydrocolloids* **2003**, *17*, 855−861.

(40) Surana, R.; Pyne, A.; Rani, M.; Suryanarayanan, R. Measurement of enthalpic relaxation by differential scanning calorimetry−effect of experimental conditions. *Thermochim. Acta* **2005**, *433*, 173−182.

(41) Yu, L.; Christie, G. Measurement of starch thermal transitions using differential scanning calorimetry. *Carbohydr. Polym.* **2001**, *46*, 179−184.

(42) Roos, Y. Characterization of food polymers using state diagram. *J. Food Eng.* **1995**, *24* (3), 339−360.

(43) Shamblin, S. L.; Taylor, L. S.; Zografi, G. Mixing behavior of colyophilized binary system. *J. Pharm. Sci.* **1998**, *87* (6), 694−701.

(44) Gordon, M.; Taylor, J. S. Ideal co-polymers and the second-order transitions of synthetic rubbers 1. Non-crystalline co-polymers. *J. Appl. Chem.* **1952**, *2*, 493−500.

(45) Simha, R.; Boyer, R. F. On a general relation involving the glass temperature and coefficients of expansions of polymers. *J. Chem. Phys.* **1962**, *37*, 1003−1007.

(46) Truong, V.; Bhandari, B. R.; Howes, T.; Adhikari, B. Analytical model for the prediction of glass transition temperature of food systems. In *Amorphous Food and Pharmaceutical Systems*; Levine, H., Ed.; Royal Society of Chemistry: Cambridge, U.K., 2002; pp 31−47.

(47) Shamblin, S. L.; Huang, E. Y.; Zografi, G. The effect of colyophilized polymeric additives on the glass transition temperature and crystallization of amorphous sucrose. *J. Therm. Anal.* **1996**, *47*, 1567−1579.

(48) Lopez, E. C.; Champion, D.; Blond, G.; Le Meste, M. Influence of dextran, pullulan, and gum arabic on the physical properties of frozen sucrose solution. *Carbohydr. Polym.* **2005**, *59*, 83−91.

(49) Gabarra, P.; Hartel, R. W. Corn syrup solids and their saccharide fractions affect crystallization of amorphous sucrose. *J. Food Sci.* **1998**, *3* (3), 523−528.

(50) Kets, E. P. W.; IJpelaar, P. J.; Hoekstra, F. A.; Hromans, H. Citrate increase glass transition temperature of vitrified sucrose preparations. *Cryobiology* **2004**, *48*, 46−54.

(51) Kilburn, D.; Claude, J.; Mezzenga, R.; Dlubek, G.; Alam, A.; Ubbink, J. Water in glassy carbohydrates: opening it up at the nanolevel. *J. Phys. Chem. B* **2004**, *108*, 12436−12441.

(52) Bizot, H.; Lebail, P.; Leroux, B.; Davy, J.; Roger, P.; Buleon, A. Calorimetric evaluation of glass transition in hydrated, linear and branched polyanhydroglucose compounds. *Carbohydr. Polym.* **1997**, *32*, 33−50.
(53) Peleg, M. Description of mechanical changes in foods at their glass transtion region. In *Food Preservations by Moisture Control: Fundamentals and Applications*; Barbosa-Canovas, Q. V., Welti-Chanes, J., Eds.; Technomic Publishing: Lancaster, PA, 1995; pp 659−671.
(54) Yoshida, H. Relationship between enthalpy relaxation and dynamic mechanical relaxation of engineering plastics. *Thermochim. Acta* **1995**, *266*, 119−127.
(55) Montes, H.; Mazeau, K.; Cavaille, J. Y. The mechanical β relaxation in amorphous cellulose. *J. Non-Cryst. Solids* **1998**, *235*−*237*, 416−421.
(56) Noel, T.; Parker, R.; Ring, S. G. A comparative study of dielectric relaxation behaviour of glucose, maltose, and their mixtures with water in liquid and glassy states. *Carbohydr. Res.* **1996**, *282*, 193−206.
(57) Moynihan, C. T.; Easteal, A. J.; Debolt, M. A. Dependence of fictive temperature of glass on cooling rate. *J. Am. Ceram. Soc.* **1976**, *59*, 12−16.
(58) Montserrat, S. Physical ageing studies in epoxy resin. I. Kinetics of the enthalpy relaxation process in a fully cured epoxy resin. *J. Polym. Sci.: Part B: Polym. Phys.* **1994**, *32*, 509−522.
(59) Hancock, B. C.; Shamblin, S. L.; Zografi, G. Molecular mobility of amorphous pharmaceutical solids below their glass transition temperatures. *Pharm. Res.* **1995**, *12*, 799−806.
(60) Hodge, I. M. Enthalpy relaxation and recovery in amorphous materials. *J. Non-Cryst. Solids* **1994**, *169*, 211−266.
(61) Lammert, A. M.; Lammert, R. M.; Schimidt, S. J. Physical aging of maltose glasses as measured by standard and modulated differential scanning calorimetry. *J. Therm. Anal. Calorim.* **1999**, *55*, 949−975.
(62) Truong, V.; Bhandari, B. R.; Howes, T.; Adhikari, B. Physical aging of amorphous fructose. *J. Food Sci.* **2002**, *26* (8), 3011−3018.

Received for review January 21, 2006. Revised manuscript received June 15, 2006. Accepted June 16, 2006. Academic Research Grant R-143-000-216-112 from the National University of Singapore is gratefully acknowledged.

JF060188R